# Magnetic Circular Dichroism of Resonant X-Ray Emission Spectroscopy Related to Er $2p \rightarrow 4f$ Electric Quadrupolar Transition in $Er_3Fe_5O_{12}$

Naomi Kawamura*, Masaichiro Mizumaki*, Hiroshi Maruyama† and Testuya Ishikawa**,*

*JASRI/SPring-8, 1-1-1 Kouto, Sayo, Hyogo 678-5198, JAPAN
†Hiroshima Univ., 1-3-1 Kagamiyama, Higashi-Hiroshima 739-8526, JAPAN
**RIKEN/SPring-8, 1-1-1 Kouto, Sayo, Hyogo 679-5148, JAPAN

**Abstract.** For $Er^{3+}$ ion in $Er_3Fe_5O_{12}$, magnetic circular dichroism (MCD) of X-ray emission spectra (XES) have been recorded in the pre-edge region of the Er $L_3$-absorption edge. The XES-MCD spectrum, consisting of the main peaks and their satellites, drastically varies with the incident angle of X-ray. The angle-dependent spectrum shows that the satellite structure originates from the electric quadrupolar $2p \rightarrow 4f$ transition. The experimental result is compared with a theoretical calculation based on the atomic model.

**Keywords:** Electric quadrupolar transition, Erbium iron garnets, Resonant X-ray emission spectroscopy, Magnetic circular dichroism, Longitudinal and transverse geometries
**PACS:** 78.70.Dm, 78.70.En, 87.64.Ni

## INTRODUCTION

Electric quadrupolar (E2) transitions have been discussed for a long time in X-ray absorption spectroscopy (XAS). For the *L*-edge of rare-earth (*R*) element, it has been expected that the $2p \rightarrow 4f$ E2 excitation is located in the pre-edge region due to the strong Coulomb interaction between $2p$ core hole and $4f$ electrons. However, E2 excitations are usually obscured by a prominent absorption of the so-called white-line resulting from the $2p \rightarrow 5d$ electric dipolar (E1) excitation. This limitation is improved by X-ray magnetic circular dichroism (MCD) measurement, in which some dichroic structures have been additionally observed as low-lying spectrum in the pre-edge region. Although many XAS-MCD experiments and calculations have been made to examine the E2 excitations [1, 2, 3], there seems no wide consensus even now.

One of the effective methods to verify the E2 excitation may be X-ray emission spectroscopy (XES) that is capable of separating the E2 contribution from the E1 one due to the optical process specified by the energy of emitted photons. Bartolomé *et al.* have recorded the $R$ $3d$ or $4d \rightarrow 2p$ XES at the pre-edge of $L_3$-absorption in $R_2Fe_{14}B$ system, and they have showed that the E2 contribution is associated with the number of $4f$ electrons and consistent with the XAS-MCD data [4]. However, there have been only a few XES-MCD experiments to observe the E2 contiribution so far [5, 6], though the dichroic spectrum in XES can provide detailed information about the $R$ $4f$ electronic states. Fukui and Kotani have theoretically shown that the E2 component could be specified from the dependence of XES-MCD intensity on the incident and emitted angles of X-rays [7].

In this paper, we present Er $3d \rightarrow 2p_{3/2}$ XES-MCD spectrum in $Er_3Fe_5O_{12}$ with several different angles of the incident X-ray. The observed angle-dependent spectrum is compared with the calculated ones; consequently, the E2 transition is specified without ambiguity.

## EXPERIMENTAL

The experiment was performed on BL39XU of SPring-8. Linearly polarized X-rays were monochromatized by a Si 111 double-crystal, and were converted into the circularly polarized beam by using a diamond X-ray phase retarder of 0.73 mm in thickness. A Pt-coated mirror functioned to eliminate the higher harmonics and to focus horizontally the X-ray beam on the sample. Overall energy resolution was estimated to be 1.1 eV.

$Er_3Fe_5O_{12}$ (Er-iron garnet: Er-IG) polycrystalline was loaded into a closed-cycle He-gas refrigerator and kept at about 20 K. The applied magnetic field was fixed to 0.6 T. Angles of incident and scattered X-rays, $\theta_1, \theta_2$, are defined to the direction of sample magnetization (parallel to the magnetic field), as schematically shown in Figure 1. The X-rays emitted from the sample were analyzed by a cylindrically bent Ge 440 crystal and monitored by a position-sensitive proportional counter

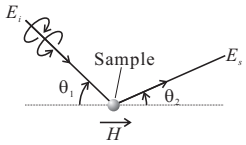


**FIGURE 1.** Definition of the angles of incident and scattered X-rays, $\theta_1$ and $\theta_2$.

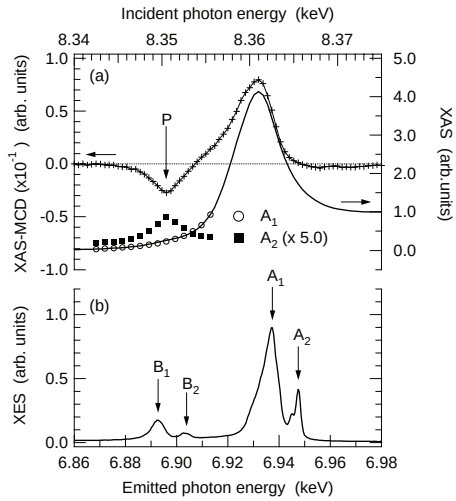


**FIGURE 2.** (a) XAS (solid line) and XAS-MCD (cross) spectra at the Er $L_3$-edge in Er-IG, and (b) Er $3d \rightarrow 2p$ XES spectrum at the incident energy 8.3505 keV. Open circles and closed squares denote the $A_1$ and $A_2$ peak intensity as a function of the incident energy, respectively.

flowing with PR gas (Ar 90% + CH4 10%).

XES-MCD spectrum is defined as a difference between the emission spectra, when the incident X-rays have plus or minus helicity. The helicity was alternated every 100 sec, and the polarity of the magnetic field was changed for every 2 hours to confirm the reversality of XES-MCD signal. To obtain a better statistics, the spectrum was accumulated for $8 \sim 16$ hours.

## RESULTS AND DISCUSSION

Figure 2 (a) shows the XAS and XAS-MCD spectra at the Er $L_3$-edge in Er-IG at $T \simeq 20$ K under $H = 0.6$ T. The XAS-MCD is mainly composed of a negative and a positive profile. According to the previous considerations, the negative part (labeled P) located in the pre-edge region is possibly assigned to the E2 contribution, which reaches to a maximum value of 2.7% at the incident photon energy $E_i(\mathrm{P}) = 8.3505$ keV. When the incident energy is tuned to $E_i(\mathrm{P})$, the XES spectrum is shown in Fig. 2 (b). The XES spectrum is composed of two main peaks of

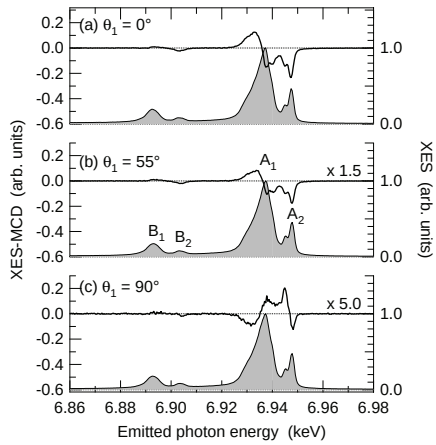


**FIGURE 3.** Er $3d \rightarrow 2p$ XES and XES-MCD spectra in the different configurations, (a) $\theta_1 = 0°$, (b) $\theta_1 = 55°$, and (c) $\theta_1 = 90°$. The scattering angle is fixed to $\theta_2 = 55°$.

$3d_{5/2} \rightarrow 2p_{3/2}$ ($L\alpha_1$-line, labeled $A_1$) and $3d_{3/2} \rightarrow 2p_{3/2}$ ($L\alpha_2$-line, labeled $B_1$) de-excitations, originating from the spin-orbit interaction of $3d$ states. In addition, two satellite peaks $A_2$ and $B_2$ are observed at higher energy side of each main peak. When the incident energy $E_i$ is increased, the $A_1$ and $B_1$ intensities are intensified and follow the XAS spectrum, whereas the $A_2$ and $B_2$ peaks have a meaningful intensity only in the pre-edge region. The different behavior between the $A_1$ and $A_2$ peaks is illustrated in Fig. 2 (a). Therefore, we consider that these $A_2$ and $B_2$ satellite peaks are attributable to the E2 transition. It is also speculated that the satellite structure reflects an energy separation due to the $3d$–$4f$ intra-atomic exchange interaction, i.e. the $3d^9$ core state with parallel (antiparallel) spin configuration to the $4f^{11}$ ($Er^{3+}$) state is situated at lower (higher) energy [8].

In order to verify this interpretation, we have recorded the XES-MCD spectrum with the different incident angle $\theta_1$ at $E_i(\mathrm{P}) = 8.3505$ keV. Figure 3 (a) $\sim$ (c) shows the XES-MCD spectrum at the incident angle $\theta_1 = 0°$, $55°$, and $90°$ under the fixed scattering angle $\theta_2 = 55°$ in comparison with the normalized XES spectrum. The MCD signal is clearly observed in a range of each peak of the XES spectrum. In the case of $(\theta_1, \theta_2) = (0°, 55°)$, the dichroic spectrum forms a positive-to-negative profile at the $A_1$ main peak and a negative double-peak profile at the $A_2$ satellite, as seen in Fig. 3 (a). Although the XES spectrum shows hardly any variation among the three configurations, the XES-MCD spectrum reveals a remarkable difference. In particular, it should be noted that the XES-MCD signal is observable even in the transverse geometry $(\theta_1, \theta_2) = (90°, 55°)$, see Fig. 3 (c). In principle, the dichroic effect in XAS is not observable in the geometry of magnetization being perpendicular to

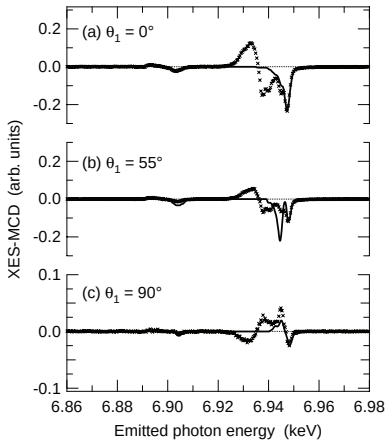


**FIGURE 4.** Comparison between the experimental result (cross) and the calculated one (solid line) for the E2 excitation in the Er $3d \rightarrow 2p$ XES-MCD spectrum in the different configurations, (a) $\theta_1 = 0°$, (b) $\theta_1 = 55°$, and (c) $\theta_1 = 90°$ [10].

the incident X-ray wave vector. Hence, the XES-MCD in the transverse geometry could be caused by the quantum mechanical interference effect, which has been explained by Fukui *et al.* [9].

When the incident angle $\theta_1$ increases, the main $A_1$ and $B_1$ peaks reduce the XES-MCD intensity, and its sign reverses in an intermediate range of $\theta_1 = 55° \sim 90°$. This result is consistent with the theoretical calculation based on the E1 excitation [9]. On the other hand, the satellite $A_2$ peak shows a peculiar behavior; that is, a part of the double-peak changes the sign from negative to positive, while the other part remains the original negative sign. This drastic variation of the satellite peak results from the $\theta_1$ dependence of both the diagonal and interference terms in the transition matrix elements for the E2 excitation, and it is different from the variation for the E1 excitation [7].

Fukui *et al.* have made preliminary calculations of the XES-MCD spectrum depending on $\theta_1$ for the $2p \rightarrow 4f$ E2 transition [10]. Figure 4 shows the calculated result in comparison with our experimental result. The calculated result partly reproduces our present observations about the satellite $A_2$ and $B_2$ peaks. Hence, it is confirmed that the E2 transition contributes to the dichroic effect in the pre-edge region. Quantitatively, however, the calculated intensity ratio is still in poor agreement with the experiment. The discrepancy may be ascribed to the influence of the strong E1 contribution. In order to explain the discrepancy, it is necessary to perform a detailed theoretical calculation for $Er^{3+}$ ion including the E1 transition. The $2p \rightarrow 4f$ E2 excitation is specified as the satellite of the $L\alpha_{1,2}$-XES peak in the pre-edge region of XAS spectrum.

## CONCLUSION

The XES and XES-MCD spectra have been successfully recorded at the Er $L_3$ pre-edge region with different angles of the incident X-ray. We have observed the main peak and satellites in the XES-MCD spectrum, which are modified between longitudinal and transverse geometries. The present result is compared with theoretical calculations and it is concluded that the satellite of the $L\alpha_{1,2}$-XES peak originates from the $2p \rightarrow 4f$ quadrupolar transition. The XES-MCD experiment is a useful tool for studying the $4f$ electronic states through the $3d$–$4f$ intra-atomic exchange interaction.

## ACKNOWLEDGMENTS

The authors acknowledge Drs. M. Nakazawa and K. Fukui, and Prof. A. Kotani for their theoretical discussions. This study was performed with the approval of the Japan Synchrotron Radiation Research Institute (JASRI) (Proposal No. 2002A0101-NS2-np and 2002B0254-CS2-np).

## REFERENCES

1. J. C. Lang, S. W. Kycia, X. D. Wang, B. N. Harmon, A. I. Goldman, D. J. Branagan, R. W. McCallum and K. D. Finkelstein, *Phys. Rev.*, **B46**, 5298–5302 (1992).
2. K. Shimomi, H. Maruyama, K. Kobayashi, A. Koizumi, H. Yamazaki and T. Iwazumi, *Jpn. J. Appl. Phys.*, Suppl. **32-2**, 314–316 (1993).
3. J. Chaboy, F. Bartolomé, L. M. García and G. Cibin, *Phys. Rev.*, **B57**, R5598–R5601 (1998).
4. F. Bartolomé, M. Krisch, D. Raoux and J. M. Tonnerre, *Phys. Rev.*, **B60**, 13497–13506 (1999).
5. T. Iwazumi, K. Kobayashi, S. Kishimoto, T. Nakamura, S. Nanao, D. Ohsawa, R. Katano and Y. Isozumi, *Phys. Rev.* **B56**, R14267–R14270 (1997).
6. T. Nakamura, H. Shoji, E. Hirai, S. Nanao, K. Fukui, H. Ogasawara, A. Kotani, T. Iwazumi, I. Harada, R. Katano and Y. Isozumi, *Phys. Rev.* **B67**, 094439-1–7 (2003).
7. K. Fukui and A. Kotani, *J. Phys. Soc. Jpn.* **73**, 1059–1064 (2004).
8. M. Nakazawa, and K. Fukui, H. Ogasawara, A. Kotani and C. F. Hague, *Phys. Rev.* **B66**, 113104-1–4 (2002).
9. K. Fukui, H. Ogasawara, A. Kotani, T. Iwazumi, H. Shoji, and T. Nakamura, *J. Phys. Soc. Jpn.* **70**, 3457–3463 (2001).
10. K. Fukui, M. Nakazawa and A. Kotani, *Private communication*.